ELSEVIER

Journal of Alloys and Compounds 303–304 (2000) 191–197

Journal of ALLOYS AND COMPOUNDS

www.elsevier.com/locate/jallcom

Synthesis and properties of colloidal lanthanide-doped nanocrystals

M. Haase*, K. Riwotzki, H. Meyssamy, A. Kornowski

Institut für Physikalische Chemie, Universität Hamburg, Bundesstraße 45, D-20146 Hamburg, Germany

Abstract

Colloidal solutions and redispersible powders of nanocrystalline, lanthanide-doped phosphates and vanadates have been prepared in high-boiling coordinating solvents or by hydrothermal means in aqueous solution. Highly crystalline materials were obtained by both methods despite the low temperature of 200°C applied during the synthesis. The materials have been characterized by using high-resolution TEM, powder-XRD, absorption spectroscopy and luminescence spectroscopy. By analyzing line splitting and intensity pattern in the luminescence spectra of the europium-doped samples, we are able to verify that the dopant ions enter the same lattice sites as in the corresponding bulk material. Size-selected samples of hydrothermally prepared lanthanide-doped YVO_4 consist of particles ranging in size from about 10 to 30 nm. The nanoparticles exhibit the tetragonal zircon structure known for bulk material. In the case of $LaPO_4$ the hydrothermal method yields nanoparticles or nano-fibers (width of about 9 nm) depending on the synthesis conditions, while the synthesis in high-boiling solvents yields colloids with a very narrow size distribution and a mean particle size of 4.5 nm. All $LaPO_4$-nanomaterials exhibit the monazite-structure, irrespective of their morphology or size. In all systems investigated, energy transfer between the host and the dopant ions is observed. Upon UV excitation, aqueous colloidal solutions of YVO_4:Eu nanoparticles show a luminescence quantum yield of 15% at room-temperature. In $LaPO_4$:Ce, Tb energy transfer is observed between cerium and terbium ions.

Keywords: Synthesis; Properties; Colloidal solutions; Lanthanides-doped phosphates/vanadates; Nanocrystals

1. Introduction

Liquid phase synthesis methods have often been utilized to prepare colloidal solutions of highly crystalline and well separated nanoparticles. Since light scattering at separated particles in the nanometer-size regime is negligible, these colloids can be investigated with the same spectroscopic techniques as used for solutions of molecules. In particular, colloids of semiconductor nanocrystallites have been investigated intensively since their spectroscopic data provide information on the electronic energy structure of the nanoparticles [1–7]. Liquid phase methods have been applied to the preparation of doped nanoparticles [8,9], too, but to a much lesser extent. The most thoroughly investigated systems are manganese-doped zinc sulfide and cadmium sulfide [10–18]. Furthermore, CdS, CdSe and ZnO nanoparticles have been prepared in the presence of erbium(3^+) by a solution synthesis [19].

Since liquid phase synthesis methods are restricted to temperatures below about 350°C, i.e. to temperatures much lower than employed in solid state reactions, one has to prove that the dopant ions do neither enter the host lattice as interstitials, nor are they deposited onto the outer surface of the particles only. Verifying that the dopant ions occupy the same sites as in bulk material, however, requires an analytical tool that is sensitive to the local environment of the dopant ion in the nanocrystalline host. A technique often applied is EXAFS spectroscopy, which was used to investigate nanocrystalline Y_20_3:Tb [20] and ZnS:Mn [21]. A few dopants are known, however, where the luminescence spectrum of the dopant ion itself can be used to probe its crystal environment. The most extensively used probe of this kind is the Eu^{3+}-ion [22] showing a luminescence line spectrum which corresponds to transitions within the manifold of f-electron states of europium. The symmetry of the europium site in the crystal lattice gives rise to a characteristic crystal field splitting of the energy levels of europium and a characteristic intensity pattern of the luminescence lines. The line spectrum of Eu^{3+} is comparatively easy to analyze since the strongest transitions originate from an energy state that is not split by the crystal field.

In this paper, we report on the solution phase synthesis of lanthanide-doped YVO_4- and $LaPO_4$-nanomaterials. Bulk YVO_4 and $LaPO_4$ have been extensively used as hosts for lanthanide ions [23,24]. The lanthanide dopant

*Corresponding author.

0925-8388/00/$ – see front matter
PII: S0925-8388(00)00628-9

substitutes for yttrium in the YVO_4 lattice and for lanthanum in the $LaPO_4$ lattice, respectively.

Bulk $LaPO_4$ doped with cerium and terbium [25,26] is a commercially applied lamp phosphor exhibiting a high luminescence quantum yield. Bulk YVO_4:Eu had been extensively used as red phosphor in cathode ray tubes, before it was replaced by the even more efficient Y_2O_2S:Eu. Bulk $LaPO_4$ and bulk YVO_4 are usually prepared by solid state reactions at temperatures above 1300 K, but hydrothermal methods have been described as well [27,28].

2. Experimental

Lanthanide-doped YVO_4 and $LaPO_4$ nanomaterials were prepared hydrothermally as reported previously [29,30]. In brief, aqueous solutions of the lanthanide nitrates (host metal and dopant) were precipitated with 1 M NaOH and the resulting suspension was combined with an aqueous solution of sodium vanadate or sodium phosphate. The suspension was adjusted to pH 12.5 and heated at 200°C for 1–2 h in a Teflon-lined autoclave with stirring. The precipitate was separated by centrifugation at $3000\times g$ for 10 min and stirred subsequently in dilute acid (nitric acid or 1-hydroxyethane-1,1-diphosphonic acid) in order to remove metal hydroxides. The solid content remaining was separated by centrifugation (10 min at $3000\times g$). Upon stirring in water the precipitate formed a colloidal solution ('peptization'). Finally, the YVO_4 and $LaPO_4$ colloids were centrifuged at $60\,000\times g$ for 10 min and at $12\,500\times g$ for 5 min, respectively. The supernatants were stored in capped vessels.

Similarly, highly acicular $LaPO_4$ was prepared by adjusting the reaction mixture given above to pH 4 instead of pH 12.5 [30].

Very small particles of doped $LaPO_4$:Eu were prepared by reacting lanthanum chloride and europium chloride with phosphoric acid in tributylphosphate at 200°C. Details of the synthesis will be given elsewhere [31].

Transmission electron micrographs of the samples were taken by using a CCD camera (Gatan, model no. 694) connected to a Philips CM 300 UT electron microscope working at 300 kV acceleration voltage.

X-ray powder diffraction patterns of nanocrystalline powders were acquired with a Philips Xpert XRD system. Rietveld analysis [32] of the XRD data was performed using PC-Rietveld plus V1.1B software (Philips) [33].

UV-Vis absorption spectra of the colloidal solutions were recorded with a Lambda 40 spectrometer (Perkin-Elmer). Photoluminescence spectra were recorded with a Spex Fluoromax 2 spectrometer having a spectral resolution of 0.5 nm. A closed cycle cooler cryostat (Leybold) was used for measurements at 15 K.

3. Results and discussion

Fig. 1 shows transmission electron micrographs (TEM) of YVO_4:Eu (Fig. 1a) and $LaPO_4$:Eu nanomaterials (Fig. 1b–d), respectively. High resolution images of the materials are shown as insets in the micrographs and display well defined lattice fringes with different spacing, indicating that all materials are highly crystalline.

Fig. 1a displays YVO_4:Eu nanoparticles prepared hydrothermally [29]. This synthesis yields particles about 10–90 nm in diameter, with the maximum of the size-distribution at about 50 nm. The particles in Fig. 1a range in size from about 10 to 30 nm since the fraction of larger particles has been reduced by centrifugation.

The same hydrothermal method can be utilized to prepare $LaPO_4$:Eu as is shown in Fig. 1b and c. The morphology of the material depends strongly on the pH during synthesis [30]. Colloids prepared in strongly alkaline solution (Fig. 1c) consist of particles ranging in size from about 10 to 50 nm whereas growth in acidic solution yields thin fibers having a width of 5–20 nm and a length varying from 200 nm to several micrometers.

Finally, part d of Fig. 1 shows $LaPO_4$:Eu prepared in the coordinating solvent tributylphosphate [31]. The particles are much smaller (4–5 nm in diameter) than those obtained by hydrothermal synthesis and their size distribution is very narrow although no size-selection technique has been applied.

The crystal phases of the nanomaterials were determined by X-ray powder diffraction (Fig. 2). The line positions in the XRD patterns of YVO_4:Eu (a) and $LaPO_4$:Eu (b, c) are found to be consistent with the tetragonal xenotime structure and the monoclinic monazite-structure, respectively, i.e. the structures known from the corresponding bulk materials.

In order to characterize the phases more precisely, we performed a Rietveld analysis of the XRD data. As is shown in Fig. 2, the experimentally obtained XRD data (crosses) are well described by the theoretical curves (solid lines) calculated by the Rietveld method [32]. For clarity, only every fourth data point of the measured curves has been plotted. The difference between the experimental and the calculated pattern is shown below each curve and is small in all cases. Small deviations are observed only in the case of $LaPO_4$:Eu prepared in tributylphosphate where proper definition of the background is difficult due to strong peak broadening.

The numerical results of the Rietveld analysis are summarized in Table 1. In all cases, the experimental XRD data are well fitted by using values for the unit cell dimensions and the atomic positions very similar to those of the corresponding bulk phase. The Rietveld analysis yields a volume-averaged mean particle size of 21 and 49 nm for hydrothermally prepared YVO_4:Eu and $LaPO_4$:Eu, respectively, and a particle size of 4.5 nm for $LaPO_4$:Eu

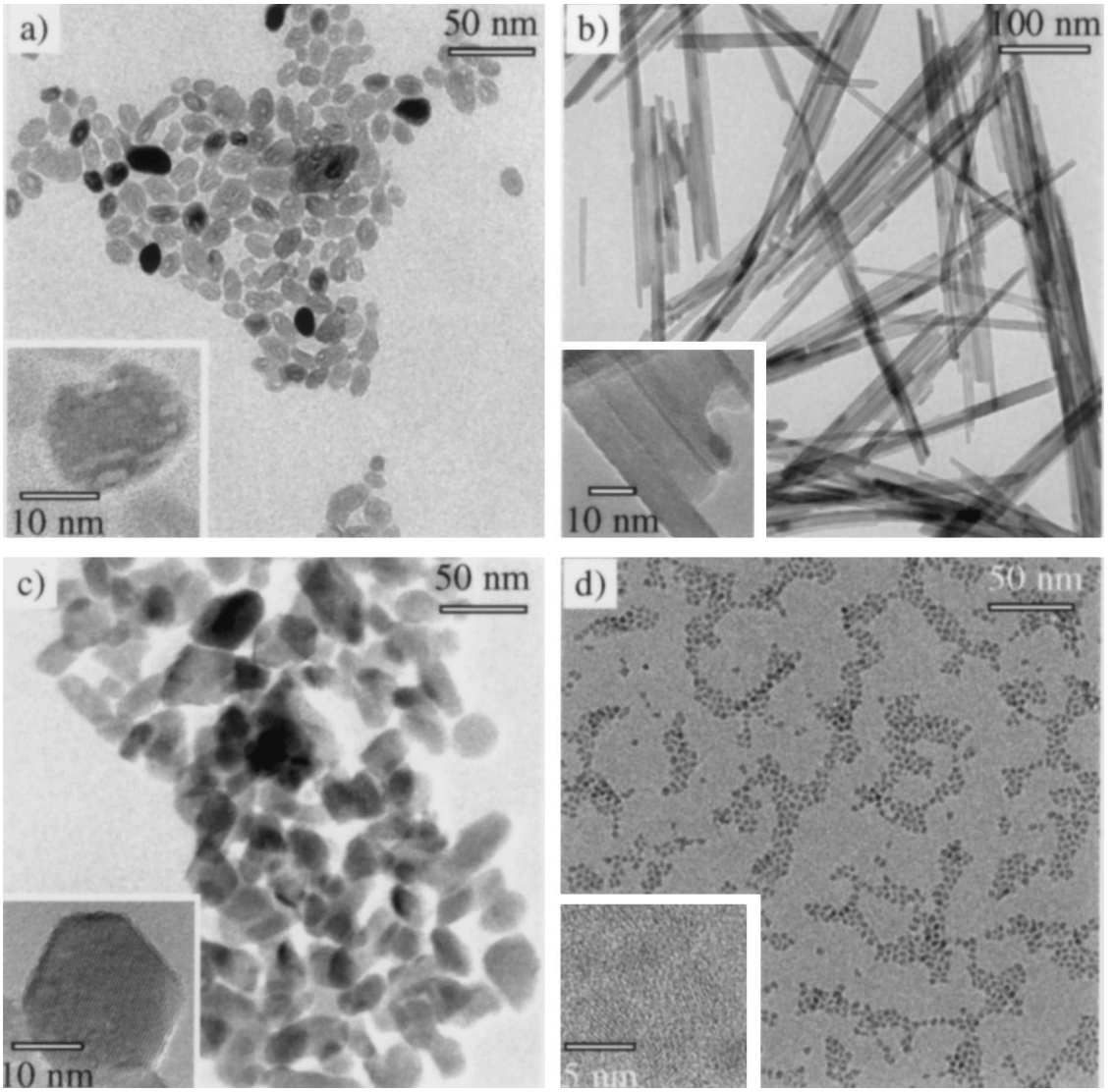

Fig. 1. TEM micrographs and high-resolution TEM images (insets) of YVO_4:Eu nanoparticles (a) and $LaPO_4$:Eu nanomaterials (b–d) prepared by solution phase synthesis methods. (a, b)YVO_4:Eu and $LaPO_4$:Eu prepared hydrothermally in acidic solution. (c) $LaPO_4$:Eu particles prepared hydrothermally in alkaline solution. (d) $LaPO_4$:Eu prepared in tributylphosphate.

prepared in tributylphosphate. These values are in accord with the particle sizes observed in the TEM images (Fig. 1).

The XRD-pattern of the $LaPO_4$:Eu fibers shows that the material crystallizes in the monazite structure, too [30]. Due to the high anisotropy of their shape, however, the width of the peaks differs strongly for the different directions in the lattice. Since the Rietveld software available cannot account for this effect, no Rietveld analysis is given for the acicular $LaPO_4$:Eu nanomaterial.

The low-temperature luminescence spectra of powders of hydrothermally prepared YVO_4:Eu and $LaPO_4$:Eu nanoparticles (Fig. 3) consist of sharp lines as expected for the transitions between europium levels, which couple only very weakly to lattice phonons. The intensity of transitions between different *J*-number levels depends on the symmetry of the local environment of the europium ion and can be described in terms of the Judd–Ofelt theory [34,35]. The splitting observed in each group of luminescence lines (Fig. 3) is caused by the crystal field. In bulk YVO_4 the Eu^{3+}-site has D_{2d} symmetry whereas the main Eu^{3+}-site in bulk $LaPO_4$ exhibits C_1 symmetry. For both materials, the splitting of the energy levels has been calculated and is in good agreement with the optical transitions actually observed in bulk YVO_4:Eu [36] and bulk $LaPO_4$:Eu [37], respectively. The theoretically expected positions [36,37] of transitions originating from the $^5D_0$ level are given in Fig. 3 as vertical lines. The figure shows that for both, nanocrystalline YVO_4:Eu and $LaPO_4$:Eu, the splitting pattern of each $^5D_0$–^7F_J transition is in accord with theory

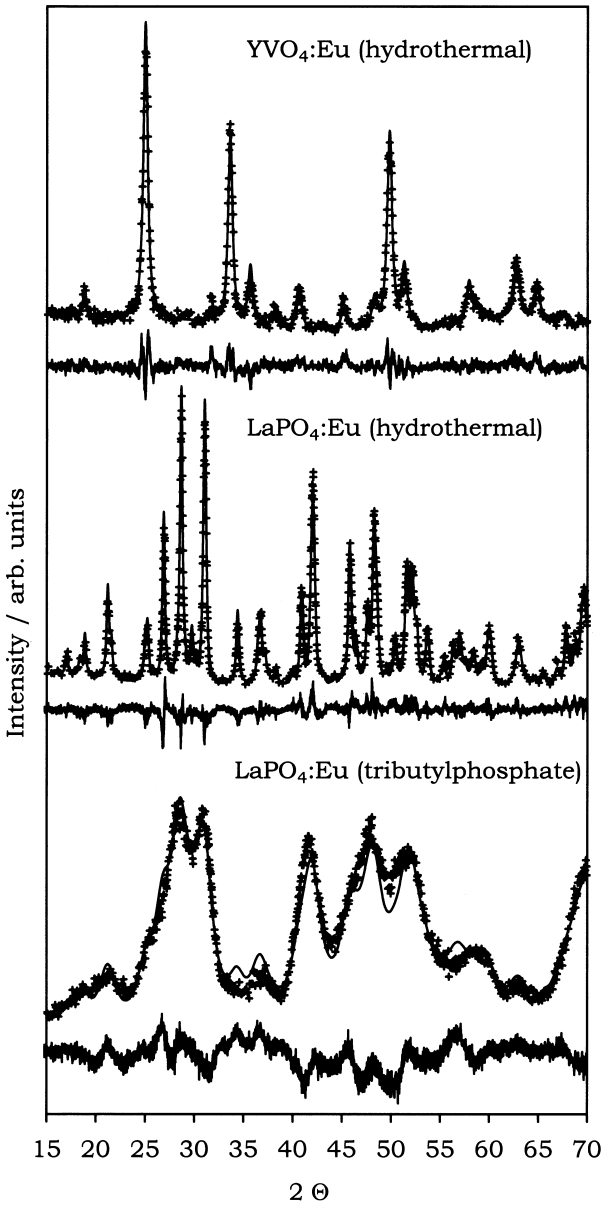

Fig. 2. X-ray powder diffraction data (+), Rietveld analysis (solid lines through data points) and difference curves of hydrothermally prepared nanoparticles of YVO_4:Eu (a), $LaPO_4$:Eu (b) and of $LaPO_4$:Eu nanoparticles prepared in tributylphosphate (c).

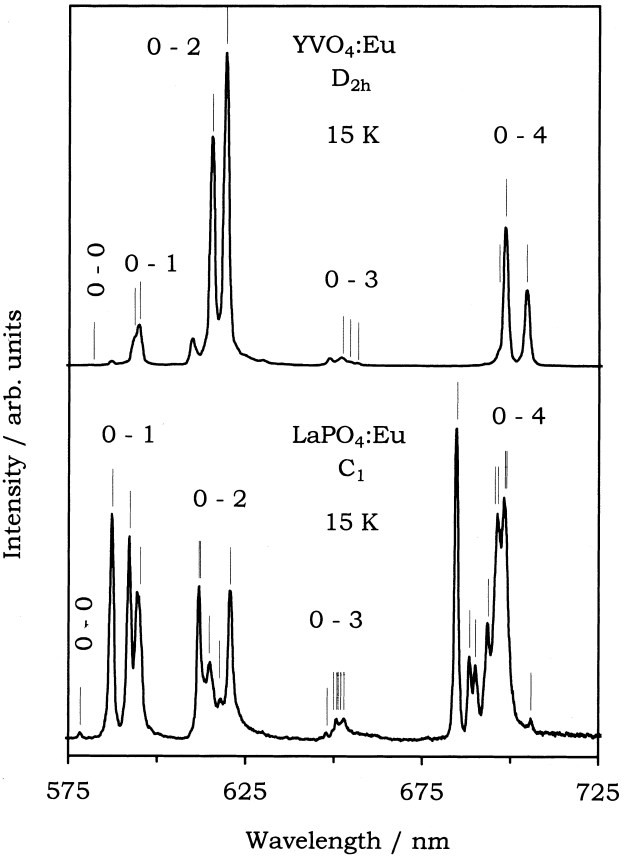

Fig. 3. Low-temperature luminescence spectra ($\lambda_{exc}=260$ nm) of hydrothermally prepared YVO_4:Eu (top) and $LaPO_4$:Eu nanoparticle powders (bottom), respectively. Main lines in both emission spectra are due to transitions from the $^5D_0$-level. Vertical lines indicate the theoretically expected positions of $^5D_0-^7F_J$ transitions.

and, hence, with the spectrum of the corresponding bulk material.

Since light scattering of colloidal particles in the nanometer size regime is negligible in dilute solution, the absorption and luminescence spectra of the particles can be measured by using their transparent colloidal solutions. The luminescence quantum yield of hydrothermally prepared YVO_4:Eu(5%) nanoparticles in colloidal solution, for instance, was determined to be 15% at room tempera-

Table 1
Numerical results of the Rietveld analysis

	YVO_4:Eu (Hydrothermal)	$LaPO_4$:Eu (Hydrothermal)	$LaPO_4$:Eu (Tributylphosphate)
Space group	*I*41/*amdZ* (141)	*P*1 21/*n*1 (14)	*P*1 21/*n*1 (14)
Unit cell parameters			
a (Å)	7.117	6.836	6.830
b (Å)	7.117	7.078	7.082
c (Å)	6.282	6.507	6.502
α (°)	90	90	90
β (°)	90	103.3	103.3
γ (°)	90	90	90
Particle size (nm)			
$\langle D\rangle_V$	21	49	4.5

ture [29]. The room temperature luminescence spectra of colloidal solutions of $LaPO_4$:Eu nanoparticles prepared by different methods are compared in Fig. 4. The figure shows that the spectrum of particles prepared in tributylphosphate (top part) is very similar to the spectrum of hydrothermally prepared particles (bottom part). Of course, the width of the luminescence lines is larger than in the low-temperature spectra shown in Fig. 3. Nevertheless, as in Fig. 3, the spectral positions of all transitions are as theoretically expected (vertical lines) for C_1-symmetry. This is a remarkable result, since europium sites with slightly different geometry may already be expected to exist due to the very large surface-to-volume ratio of the nanomaterials. If we take into account that the luminescence of an europium ion is influenced by the geometry of at least two coordination shells surrounding it, a large fraction of europium ions in a 5-nm particle is close enough to the surface that the symmetry of their sites should be affected. In the case of $LaPO_4$:Eu, however, the symmetry of the europium site is C_1 and cannot be further reduced. Eu^{3+} ions in another C_1 symmetry site may have different crystal field splittings and different relative transition intensities, but the number of crystal field levels must be the same. In bulk $LaPO_4$:Eu, three different europium C_1 symmetry sites have been identified [37]. These sites show quite different relative transition intensities, whereas the transition energies are identical within ± 20 cm^{-1}.

If we anneal hydrothermally prepared nanoparticles at 1300 K, i.e. a temperature typically employed during the solid state synthesis of the bulk materials, crystal growth takes place as it is evident from the narrowing of the X-ray diffraction lines. In fact, the low-temperature luminescence spectra (15 K) given in Fig. 5 show a change of the intensity pattern after annealing, but this effect may at least in part be caused by a preferred orientation of the nanocrystallites and a weak polarization of our excitation light. However, Fig. 5 also shows that annealing causes a narrowing of the emission lines whereas the spectral positions of the europium transitions are not altered. A broadening of the emission lines with respect to the bulk material has been observed in nanocrystalline Y_2O_3:Eu prepared by laser ablation and has been explained by an increased disorder of the europium sites in the nanomaterial [38]. This may be taken as an additional hint that europium sites with slightly different geometry exist in the nanomaterial. A more detailed analysis revealing the presence or absence of additional europium sites in our nanomaterials, however, requires use of site-selective

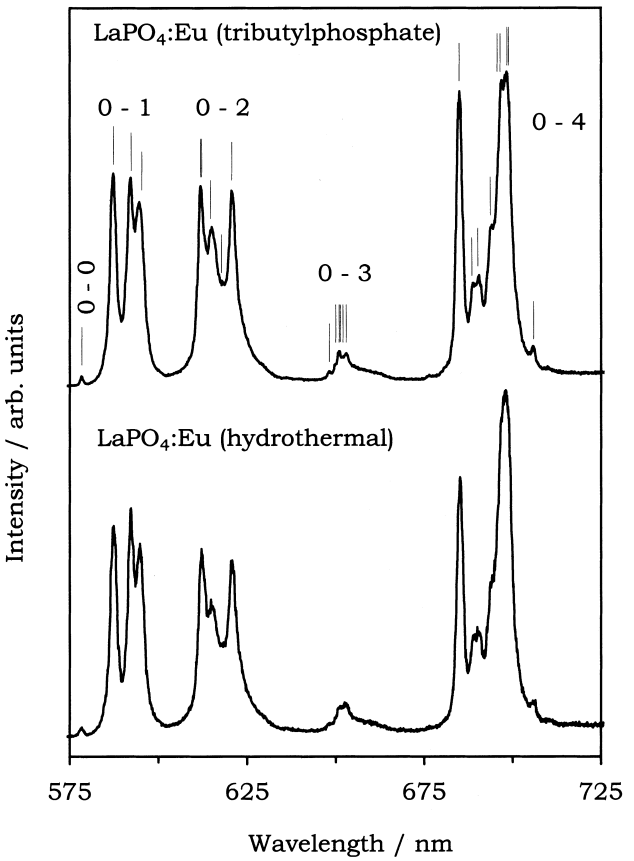

Fig. 4. Room temperature luminescence spectra ($\lambda_{exc} = 260$ nm) of colloidal solutions of nanocrystalline $LaPO_4$:Eu prepared in tributylphosphate (top) and by hydrothermal means (bottom), respectively.

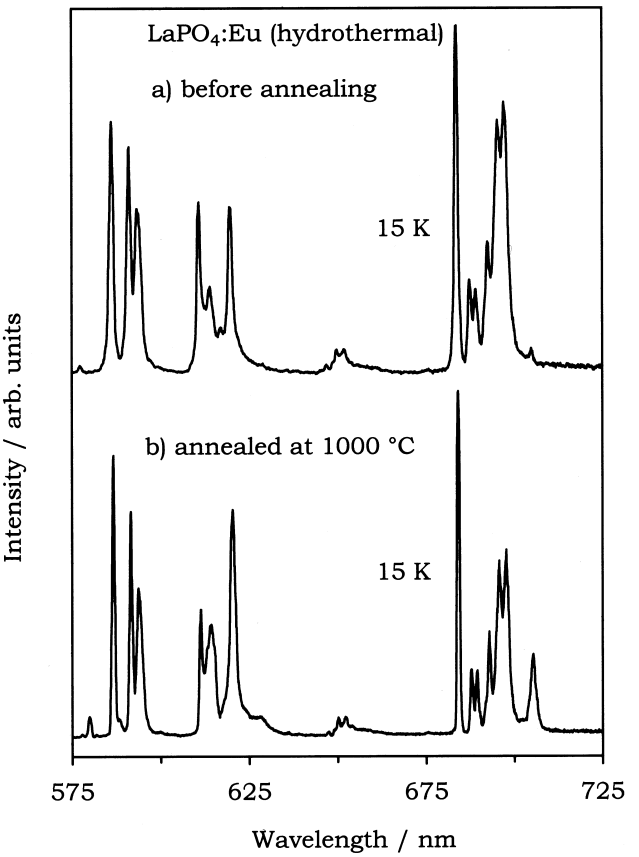

Fig. 5. Low-temperature luminescence spectra ($\lambda_{exc} = 260$ nm) of hydrothermally prepared $LaPO_4$:Eu nanoparticle powders before (upper part) and after (lower part) annealing at 1000°C.

spectroscopy methods which is beyond the scope of this study.

Fig. 6 displays the luminescence excitation spectrum (solid line) of a strongly diluted ($7 \cdot 10^{-5}$ M) YVO_4:Eu(5%)-colloid. The spectrum exhibits a peak-shape behavior in the UV, practically identical to the absorption spectrum of the colloid (broken line). The appearance of the vanadate band in the excitation spectrum shows that after optical excitation of the host, energy transfer to the Eu^{3+}-ions occurs as it is the case in bulk material [39].

The lower part of Fig. 6 shows the luminescence spectra of colloidal solutions of $LaPO_4$-fibers doped with cerium (5 mol%) (broken line) and of $LaPO_4$-fibers doped with cerium and terbium ($La_{0.40}Ce_{0.45}Tb_{0.15}PO_4$, solid line). The luminescence excitation spectrum of $LaPO_4$:Ce, Tb fibers monitored at the most intense terbium transition at 542 nm is given as a solid line between 240 and 340 nm and is identical (in this region) to that of $LaPO_4$:Ce fibers monitored at 330 nm. The latter clearly reveals that energy transfer from cerium to terbium occurs as observed in bulk $LaPO_4$:Ce, Tb [25].

4. Conclusion

We prepared colloids and redispersible powders of lanthanide doped YVO_4 and $LaPO_4$ nanoparticles at low temperatures. The highly crystalline nanoparticles exhibit the same lattice structure as the corresponding bulk materials which are commonly prepared at much higher temperatures. Upon UV excitation of the host, energy transfer to the lanthanide ions occurs and the characteristic luminescence of their f–f transitions is observed. Lanthanide-doped $LaPO_4$ nanomaterials can be prepared in three different morphologies via liquid phase synthesis methods. Successful doping is evident from the luminescence spectra of the materials. For YVO_4:Eu as well as for all $LaPO_4$:Eu nanomaterials, the Eu^{3+}-emission was used to

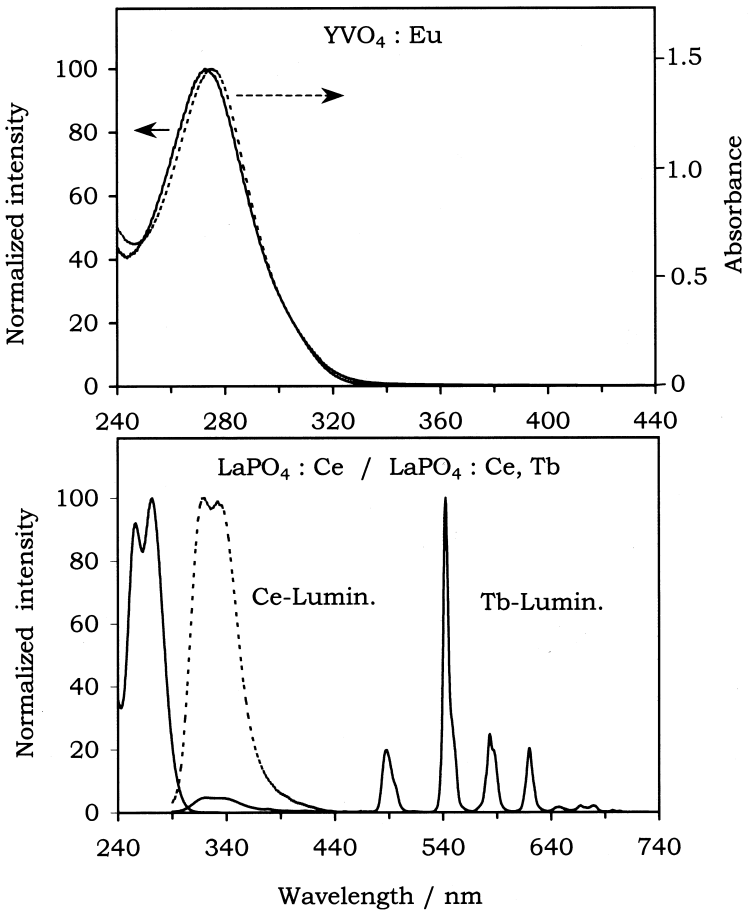

Fig. 6. Energy transfer processes in hydrothermally prepared YVO_4-nanoparticles and $LaPO_4$-nanofibers, respectively. Top part: absorption spectrum (broken line) and luminescence excitation spectrum (solid line) of a colloidal solution of YVO_4:Eu nanoparticles. Bottom part: luminescence spectrum of nanocrystalline $LaPO_4$:Ce (dashed line) and $LaPO_4$:Ce, Tb (solid line). The luminescence excitation spectrum ($\lambda_{obs} = 542$ nm) of nanocrystalline $LaPO_4$:Ce, Tb is given as a solid line in the UV region.

verify that the symmetry of the main dopant site is the same as in the corresponding bulk material. In the case of nanocrystalline $LaPO_4$:Ce, Tb energy transfer from cerium to terbium is observed.

Acknowledgements

We thank J. Ludwig and K.-H. Klaska from the Mineralogisch-Petrographisches Institut of the University of Hamburg for the measurement of the XRD spectra and for instructing us in using the Rietveld software. We greatly acknowledge funding of this project by the German Science Foundation (DFG).

References

[1] A. Henglein, Chem. Rev. 89 (1989) 1861.
[2] L.E. Brus, Appl. Phys. A 53 (1991) 465.
[3] Y. Wang, N. Herron, J. Phys. Chem. 95 (1991) 525.
[4] H. Weller, Adv. Mater. 5 (2) (1993) 88.
[5] H. Weller, A. Eychmüller, in: D.C. Neckers, D.H. Volman, G. von Bünau; (Eds.), Advances in Photochemistry, Vol. 20, Wiley, New York, 1995, p. 165.
[6] A.P. Alivisatos, J. Phys. Chem. 100 (1996) 13226.
[7] A.P. Alivisatos, Science 271 (1996) 933.
[8] R.N. Bhargava, J. Lumin. 70 (1996) 85.
[9] B.M. Tissue, Chem. Mater. 10 (1998) 2837.
[10] W.G. Becker, A.J. Bard, J. Phys. Chem. 87 (1983) 4888.
[11] D. Gallagher, W.E. Heady, J.M. Racz, R.N. Bhargava, J. Cryst. Growth 138 (1994) 970.
[12] R.N. Bhargava, D. Gallagher, X. Hong, A. Nurmikko, Phys. Rev. Lett. 72 (1994) 416.
[13] Y.L. Soo, Z.H. Ming, S.W. Huang, Y.H. Kao, R.N. Bhargava, D. Gallagher, Phys. Rev. B (Condens. Matter) 50 (11) (1994) 7602.
[14] K. Sooklal, B.S. Cullum, S.M. Angel, C.J. Murphy, J. Phys. Chem. 100 (1996) 4551.
[15] G. Counio, S. Esnouf, T. Gacoin, J.-P. Boilot, J. Phys. Chem. 100 (1996) 20021.
[16] L. Levy, J.F. Hochepied, M.P. Pileni, J. Phys. Chem. 100 (1996) 18322.
[17] L. Levy, F. Feltin, D. Ingert, M.P. Pileni, J. Phys. Chem. B 101 (1997) 9153.
[18] G. Counio, T. Gacoin, J.-P. Boilot, J. Phys. Chem. B 102 (1998) 5257.
[19] T. Schmidt, G. Müller, L. Spanhel, K. Kerkel, A. Forchel, Chem. Mater. 10 (1998) 65.
[20] Y.L. Soo, S.W. Huang, Z.H. Ming, Y.H. Kao, G.C. Smith, E. Goldburt, R. Hodel, B. Kulkarni, J.V.D. Veliadis, R.N. Bhargava, J. Appl. Phys. 83 (1998) 5404.
[21] Y.L. Soo, Z.H. Ming, S.W. Huang, Y.H. Kao, R.N. Bhargava, D. Gallagher, Phys. Rev. B (Condens. Matter) 50 (11) (1994) 7602.
[22] R.D. Peacock, Struct. Bond. 22 (1975) 83.
[23] F.C. Palilla, A.K. Levine, M. Rinkevics, J. Electrochem. Soc. 112 (8) (1965) 776.
[24] W.L. Wanmaker, A. Bril, J.W. ter Vrugt, J. Btoos, Philips Res. Rep. 21 (1966) 270.
[25] J.-C. Bourcet, F.K. Fong, J. Chem. Phys. 60 (1974) 34.
[26] N. Hashimoto, Y. Takada, K. Sato, S. Ibuki, J. Lumin. 48–49 (1991) 893.
[27] R.C. Ropp, B. Carroll, J. Inorg. Nucl. Chem. 39 (1977) 1303.
[28] Y. Hikichi, K. Hukuo, J. Shiokawa, Bull. Chem. Soc. Jpn. 51 (1978) 3645.
[29] K. Riwotzki, M. Haase, J. Phys. Chem. B 102 (1998) 10129.
[30] H. Meyssamy, K. Riwotzki, A. Kornowski, S. Naused, M. Haase, Adv. Mater. 11 (1999) 840.
[31] K. Riwotzki, H. Meyssamy, A. Kornowski, M. Haase, J. Phys. Chem. B 104 (2000), in press.
[32] R.A. Young;, The Rietveld Method, Oxford University Press, Oxford, 1993.
[33] R.X. Fischer, C. Lengauer, E. Tillmanns, R.J. Ensink, C.A. Reiss, E.J. Fantner, Mater. Sci. Forum 133–136 (1993) 287.
[34] B.R. Judd, Phys. Rev. 127 (1962) 750.
[35] G.S. Ofelt, J. Chem. Phys. 37 (1962) 511.
[36] C. Brecher, H. Samelson, A. Lempicki, R. Riley, T. Peters, Phys. Rev 155 (1967) 178.
[37] J. Dewxpert-Ghys, R. Mauricot, M.D. Faucher, J. Lumin. 69 (1996) 203.
[38] D.K. Williams, B. Bihari, B.M. Tissue, J.M. McHale, J. Phys. Chem. B. 102 (1998) 916.
[39] Ch. Hsu, C. Powell, J. Lumin. 10 (1975) 273.